Tania Ebert
University of Liverpool
For the H1 Collaboration

DIS97: Chicago, April 1997

Inclusive Jet production and Virtual Photon Structure

- Motivation
- Datasets and Monte Carlo Models
- Single Inclusive Jet Cross-Section
- Photon Remnant
- Conclusions

Motivation

- Photoproduction of high p_t jets is sensitive to parton densities in the proton and the photon.
- A quasi-real photon ($Q^2 \sim 0\,\mathrm{GeV}^2$) interacts either as a point-like object (a "direct" process) or as a partonic object (a "resolved" process).
- In deep-inelastic scattering $Q^2 >> 0\,\mathrm{GeV}^2$, the pointlike photon probes structure in the proton.

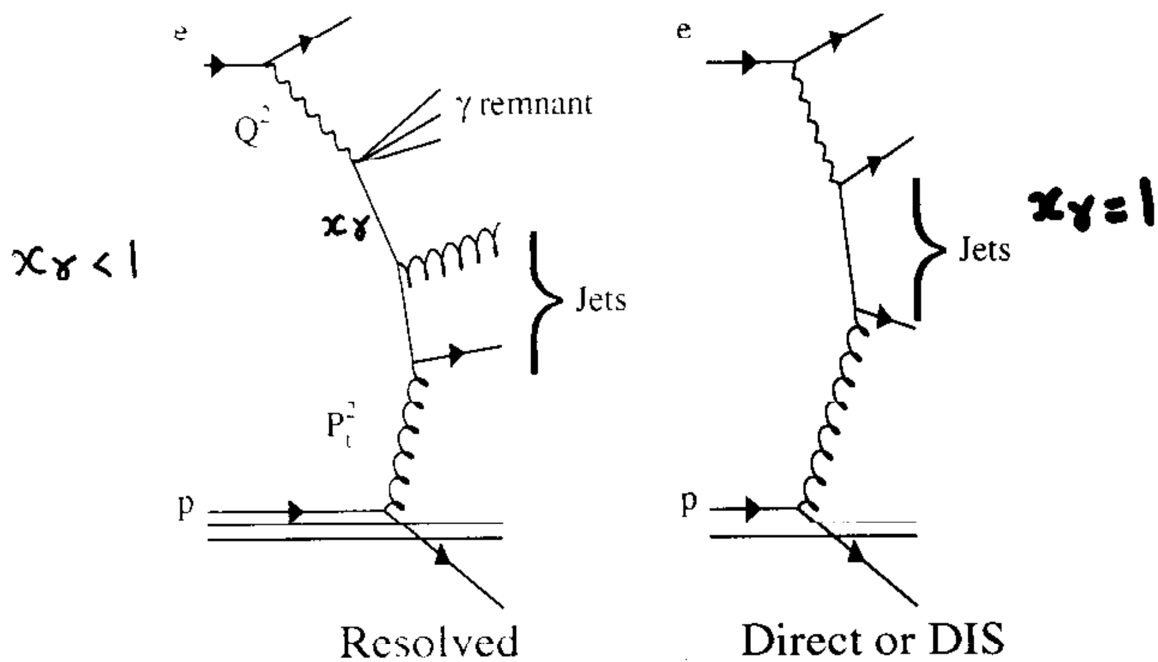

- **BUT:**
  If $Q^2 > 0\,\mathrm{GeV}^2$ and $p_t^2 >> Q^2$, the parton from the proton can probe structure inside the virtual photon.
  (transverse scale of probe << transverse dimensions of target)

- HERA *ep* data is available over a wide range of Q^2 .

- It is possible to investigate with higher statistics than measurements from e^+e^- experiments how the photon pdfs evolve with Q^2 .

- What do we expect for the structure of a virtual photon?

  - The VM piece of the cross-section varies like $\left(1/(1+\frac{Q^2}{m_v^2})\right)^2$.

  - The anomalous part of the cross-section varies like $\ln\left(\frac{p_t^2}{Q^2}\right)$

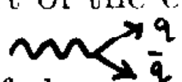

- The anomalous part of the cross-section becomes more significant as Q^2 increases.

Complications

- Multiple parton-parton interactions in resolved events

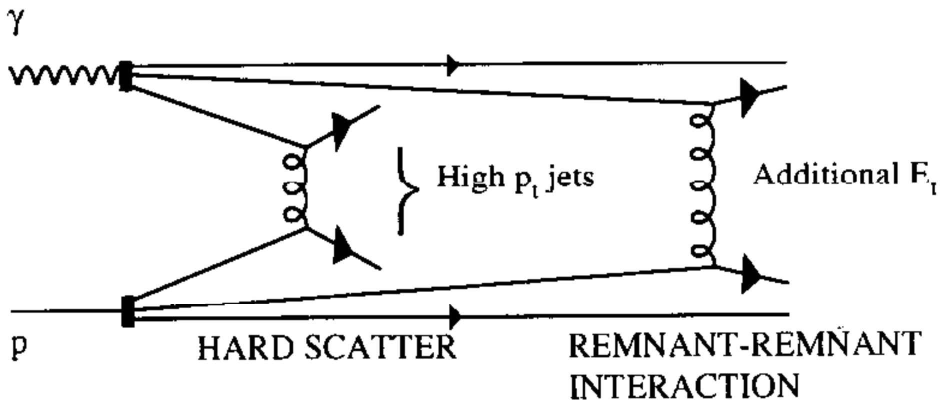

- QCD radiation (parton showers), higher order processes
  Ambiguity in distinction between direct and resolved.

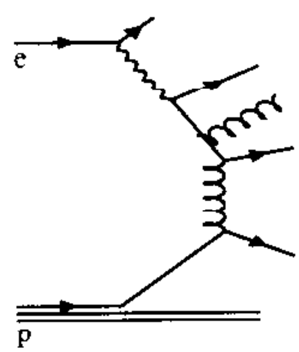

- These effects are included in Monte Carlo generators, eg HERWIG, where soft underlying event (SUE) gives additional energy uncorrelated with jets and parton showers model higher order effects.

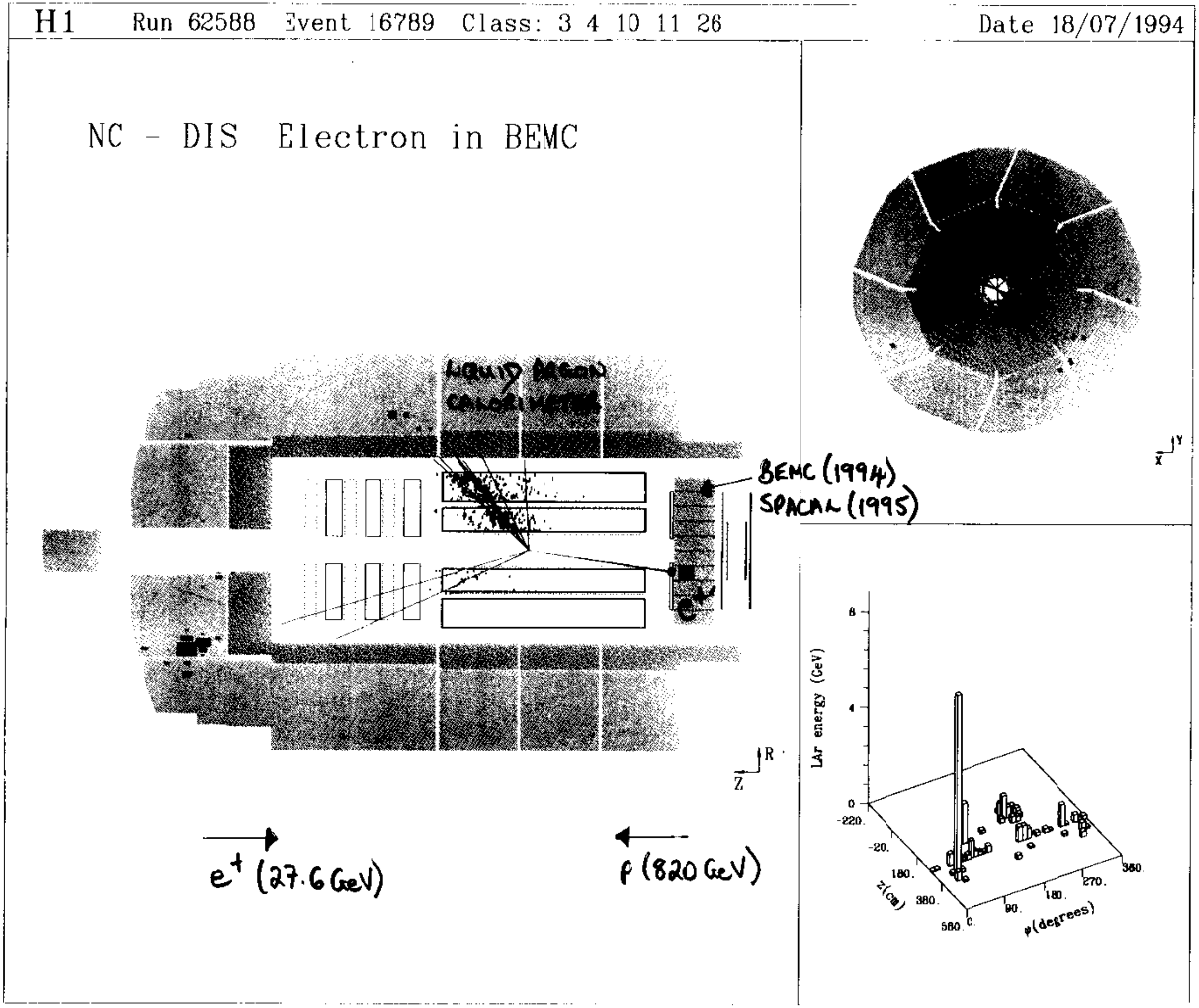

H1
Run 62588 Event 16789 Class: 3 4 10 11 26
Date 18/07/1994
NC - DIS Electron in BEMC
LIQUID ARGON CALORIMETER
BEMC (1994)
SPACAL (1995)
e+ (27.6 GeV)
p (820 GeV)
R
Z
Y
X
LAr energy (GeV)
8
4
0
-220.
-20.
180.
380.
580.
z(cm)
0
90.
180.
270.
360.
φ(degrees)

Data Selection

- Datasets:

  1. $Q^2 < 10^{-2}\,\mathrm{GeV}^2$:
     - 1994 photoproduction sample
     - Tagged electron in luminosity system
     - > 1 track pointing to vertex
  2. $0.65 < Q^2 < 20\,\mathrm{GeV}^2$:
     - 1995 shifted vertex sample
     - Interaction point shifted +70 cm
     - Identified electron in SPACAL
     - $E' > 11\,\mathrm{GeV}$
  3. $9 < Q^2 < 49\,\mathrm{GeV}^2$:
     - 1994 nominal vertex sample
     - Identified electron in BEMC
     - $E' > 11\,\mathrm{GeV}$

- Standard background suppression cuts for each dataset.

- $0.3 < y < 0.6$

Jet Reconstruction

- Jets reconstructed in $\gamma^* p$ centre of mass frame from calorimeter clusters.
- A k_t clustering algorithm was used. (c.f Catani + Webber)
- Use test variables:

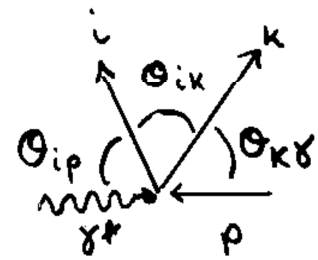

$$y_{k\gamma} = \frac{2(1-\cos\theta_{k\gamma})}{E_{cut}^2} E_k^2$$

$$y_{kp} = \frac{2(1-\cos\theta_{kp})}{E_{cut}^2} E_k^2$$

$$y_{ki} = \frac{2(1-\cos\theta_{ki})}{E_{cut}^2} \min(E_k^2, E_i^2)$$

and combine particles by addition of 4-vectors when $y < 1$.

- Particles assigned to photon and proton remnant as well as to high p_t jets.

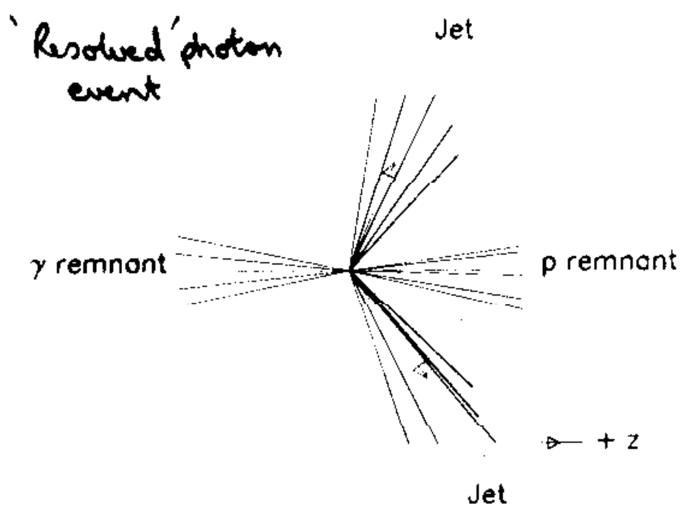

- Scale (E_{cut})=3 GeV
- Jets accepted with:
  - $E_t^* > 4(5)$ GeV for DIS (photoproduction) data
  - $-2.5 < \eta^* < -0.5$.

Phenomenological Model

- Drees and Godbole proposed a phenomenological model for a logarithmic suppression of the real photon parton densities with Q^2 .

$$\begin{aligned} f_q(x, p_t^2, Q^2) &= f_q(x, p_t^2, 0) L(p_t^2, Q^2, \omega) \\ f_g(x, p_t^2, Q^2) &= f_g(x, p_t^2, 0) L^2(p_t^2, Q^2, \omega) \\ &\text{where} \\ L(p_t^2, Q^2, \omega) &= \frac{\ln\left\{(p_t^2+\omega^2)/(Q^2+\omega^2)\right\}}{\ln\left\{(p_t^2+\omega^2)/\omega^2\right\}} \end{aligned}$$

- ω is the value of Q^2 at which the suppression becomes significant

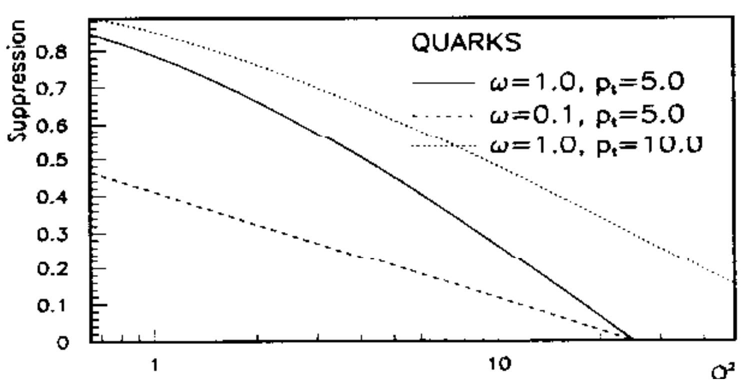

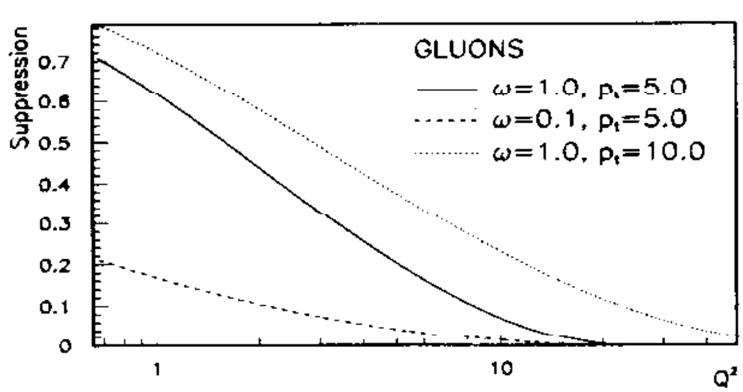

- This model is included in HERWIG 5.9.
- We use:
  - $\omega = 1\,\text{GeV}$.
  - F_2^p = GRV94 HO(DIS).
  - F_2^γ = GRV-G NLL.
  - $p_t^{min} = 1.5\,\text{GeV}$.
  - Probability of SUE = 15% for $Q^2 = 0\,\text{GeV}^2$
  - Probability of SUE = 0% for $Q^2 > 0\,\text{GeV}^2$

"HERWIG $\gamma^* p$ MODEL"

- This model gives a good description of the jet profiles.
- HERWIG Direct photon processes = BGF + QCD Compton.

Photoproduction data

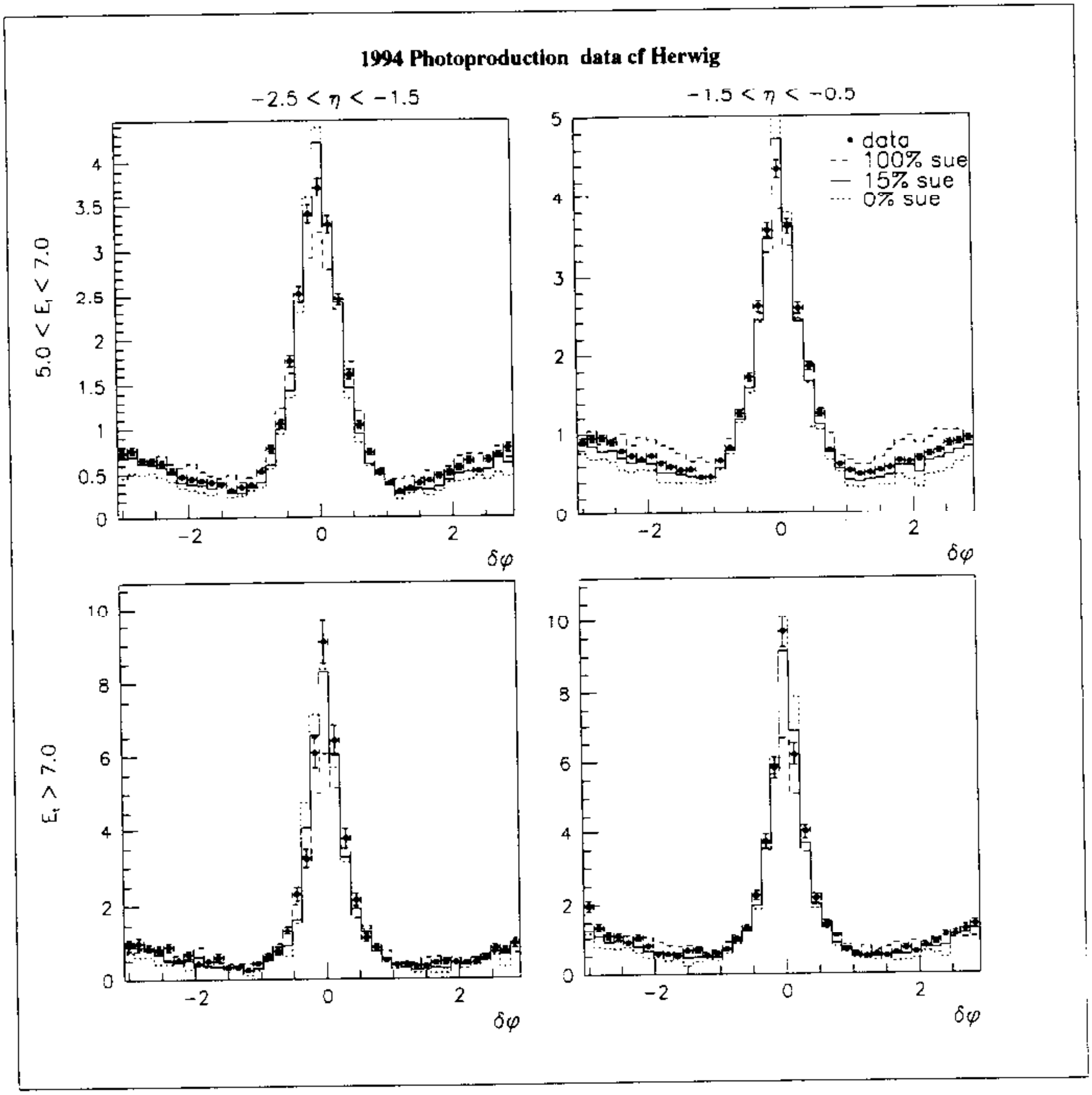

- Energy flow in ϕ around jet for $|\ \Delta\eta^*\ | < 1$
- Comparison with HERWIG direct+resolved.
- Best fit with 15% SUE for resolved processes

1995 Shifted Vertex Data

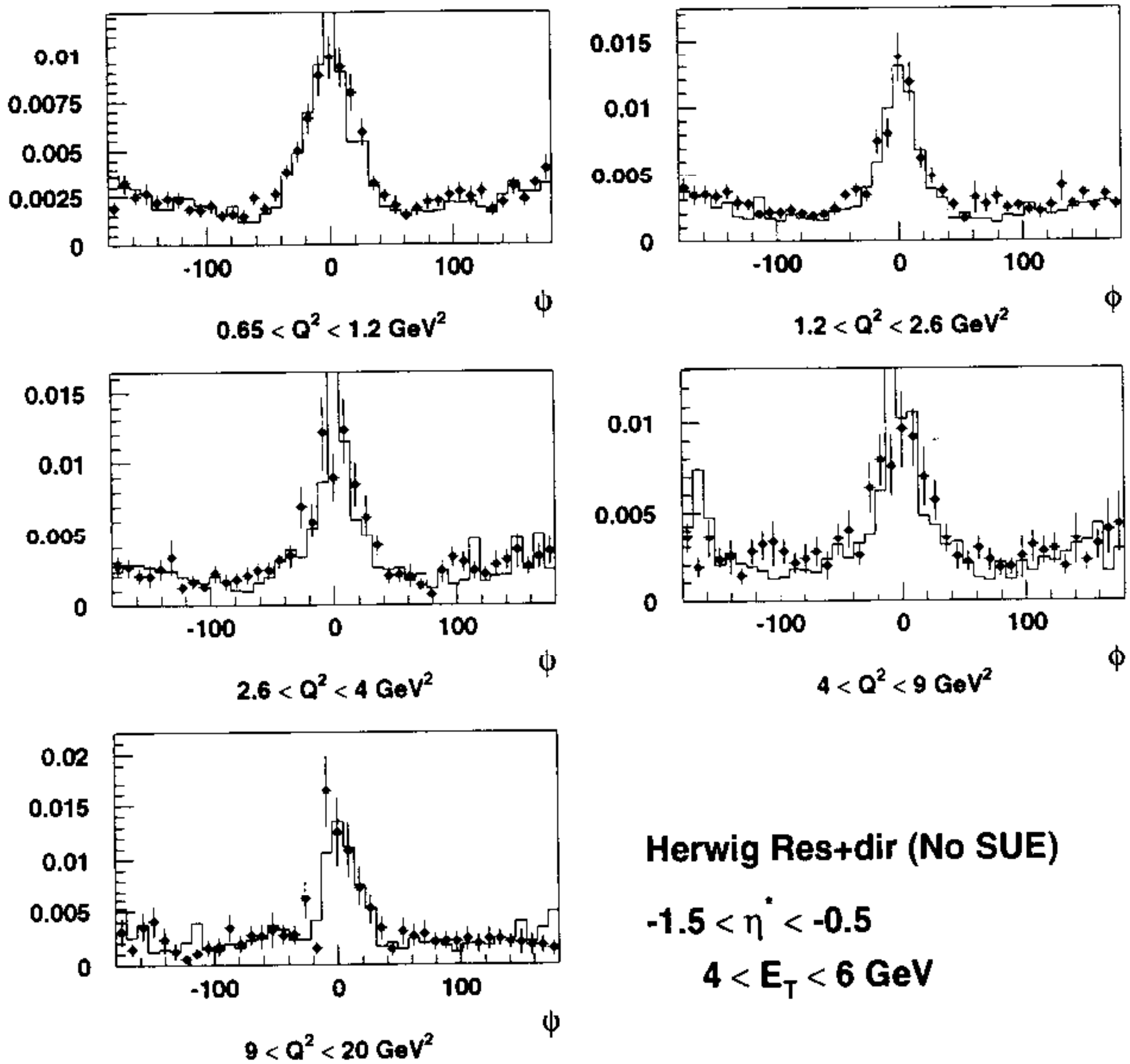

Herwig Res+dir (No SUE)

$-1.5 < \eta^* < -0.5$

$4 < E_T < 6$ GeV

- Jets with $4 < E_t^* < 6\,\mathrm{GeV}^2$ and $-1.5 < \eta^* < -0.5$.
- Energy flow in ϕ around jet for $|\Delta\eta^*| < 1$
- Comparison with HERWIG direct+resolved, no SUE

Single Inclusive Jet Cross-Sections

- Inclusive cross-section for production of jets has been measured.
- Cross-sections are presented as γ^{*}p cross-sections, defined as:

$$\sigma_{\gamma^{*}p\to e+jet+X} = \sigma_{ep\to e+jet+X}/F_{\gamma|e}$$

where:

$$F_{\gamma|e} = \int_{y_{min}}^{y^{max}} \mathrm{d}y \int_{Q^2_{min}(y)}^{Q^2_{max}} \mathrm{d}Q^2 f_{\gamma|e}(y,Q^2)$$

$$f_{\gamma|e}(y,Q^2) = \frac{\alpha}{2\pi Q^2}\left(\frac{1+(1-y)^2}{y} - \frac{2(1-y)}{y}\frac{Q^2_{min}}{Q^2}\right)$$

- Bin-by-bin correction factors determined from the HERWIG γ^{*}p model have been applied to correct for detector effects.

Systematic Errors

Error Source	γP 1994	DIS 1994	DIS 1995
Uncertainty in EM scale of BEMC/SPACAL	–	1%	2%
Uncertainty in HE scale of of BEMC/SPACAL	20%	20%	10%
Shift in electron θ	–	1 mrad	1mrad
Module-to-module uncertainty in LAr HE scale	3%	3%	3%
Uncertainty in electron tagger energy scale and resolution	1.5%	–	–

- Model dependence of the correction factors have been estimated by comparing those obtained from the HERWIG $\gamma^* p$ model with those from:
  - PHOJET for $Q^2 = 0\,\mathrm{GeV}^2$ and
  - LEPTO for $Q^2 > 0\,\mathrm{GeV}^2$.

Normalization uncertainties

- 5% uncertainty on LAr Hadronic energy scale
- 1.5(3)% error on luminosity for 1994(1995)

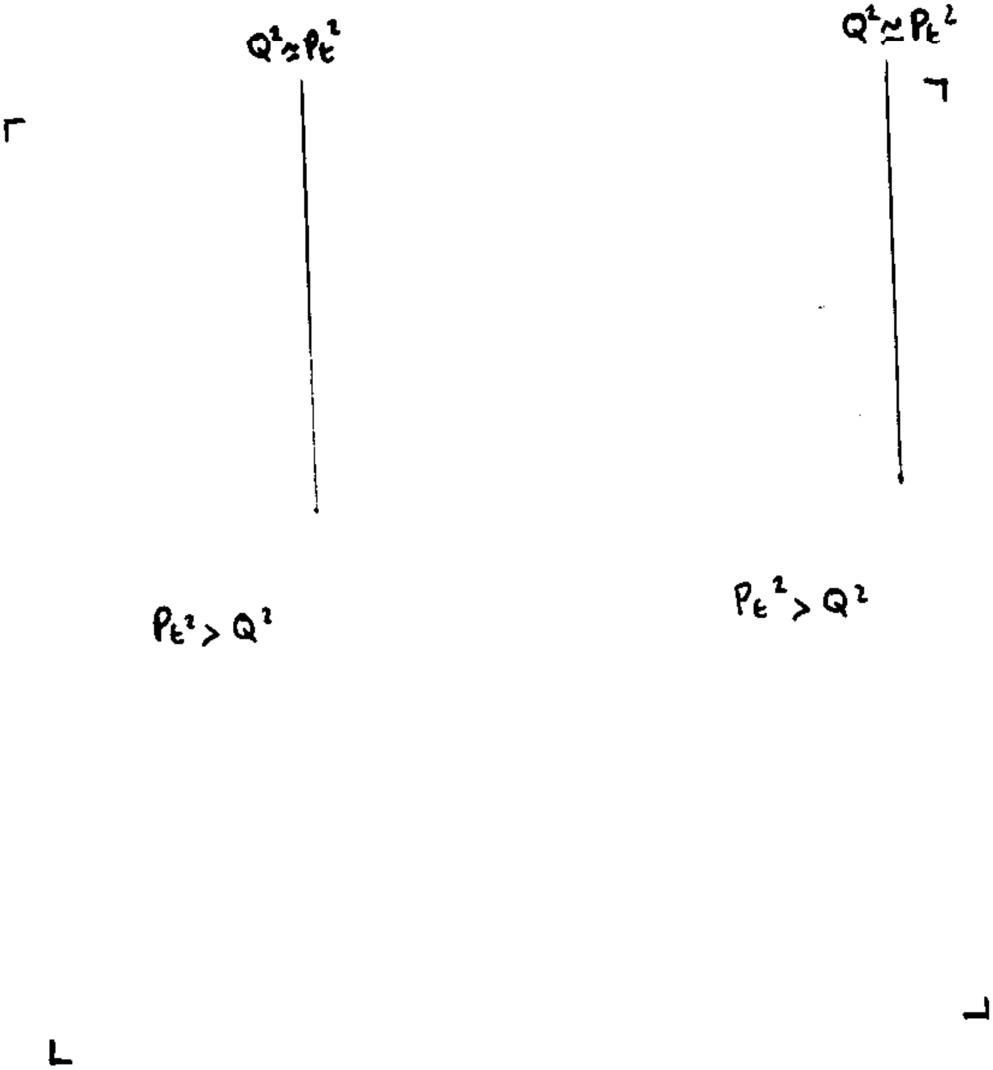

$Q^2 \simeq P_t^2$
$P_t^2 > Q^2$
$Q^2 \simeq P_t^2$
$P_t^2 > Q^2$

$$\frac{d\sigma_{\gamma^* p}}{dE_t^*}$$

- $-2.5 < \eta^* < -0.5$ and $0.3 < y < 0.6$.

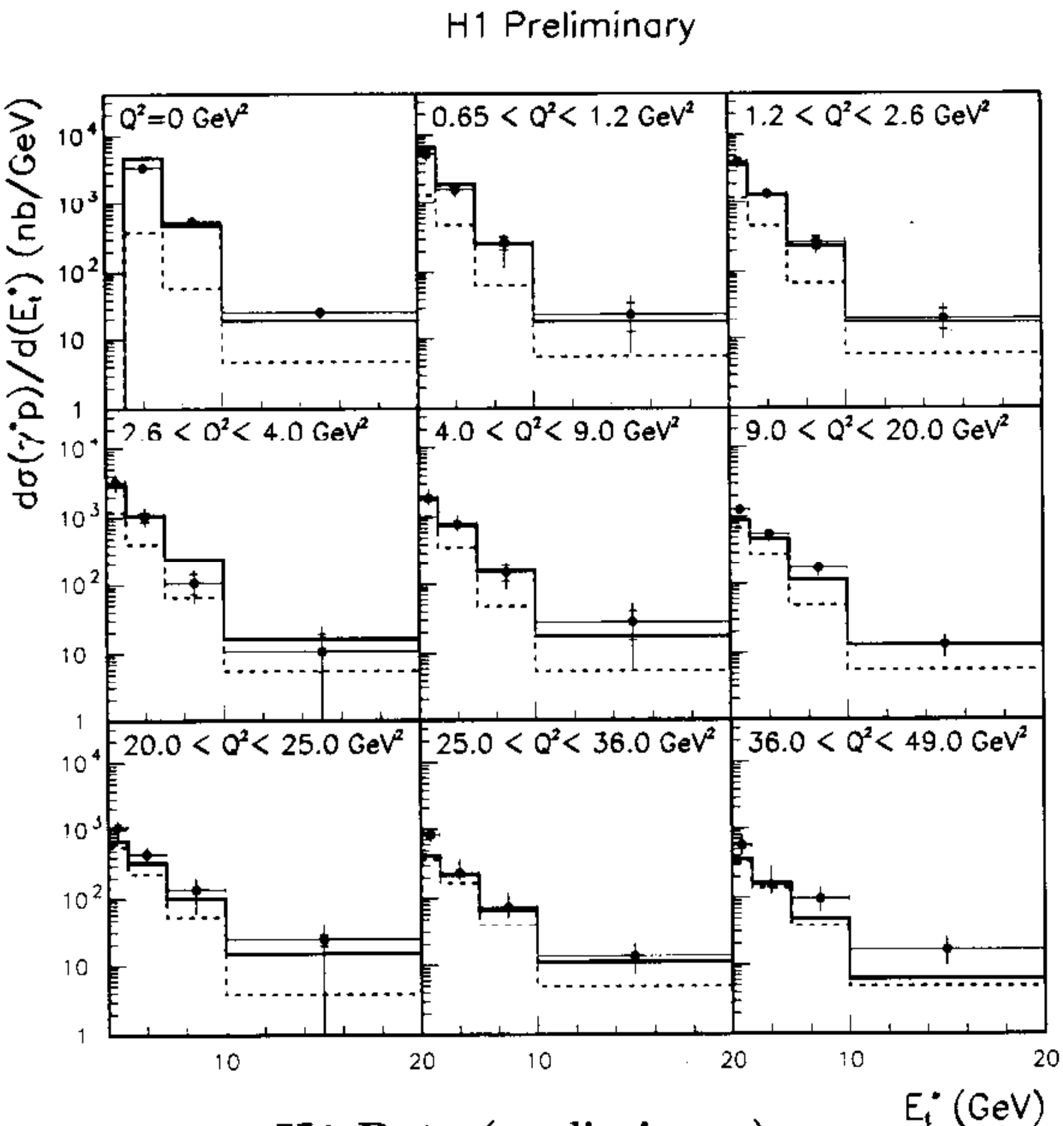

- **H1 Data (preliminary)**
- - - - HERWIG Direct
—— **HERWIG γ^*p Model (Direct+Resolved)**

- Error from Calorimeter Energy Scale shown as band.

$$\frac{d\sigma_{\gamma^* p}}{d\eta^*}$$

- $E_t^* > 5\,\mathrm{GeV}$ and $0.3 < y < 0.6$.

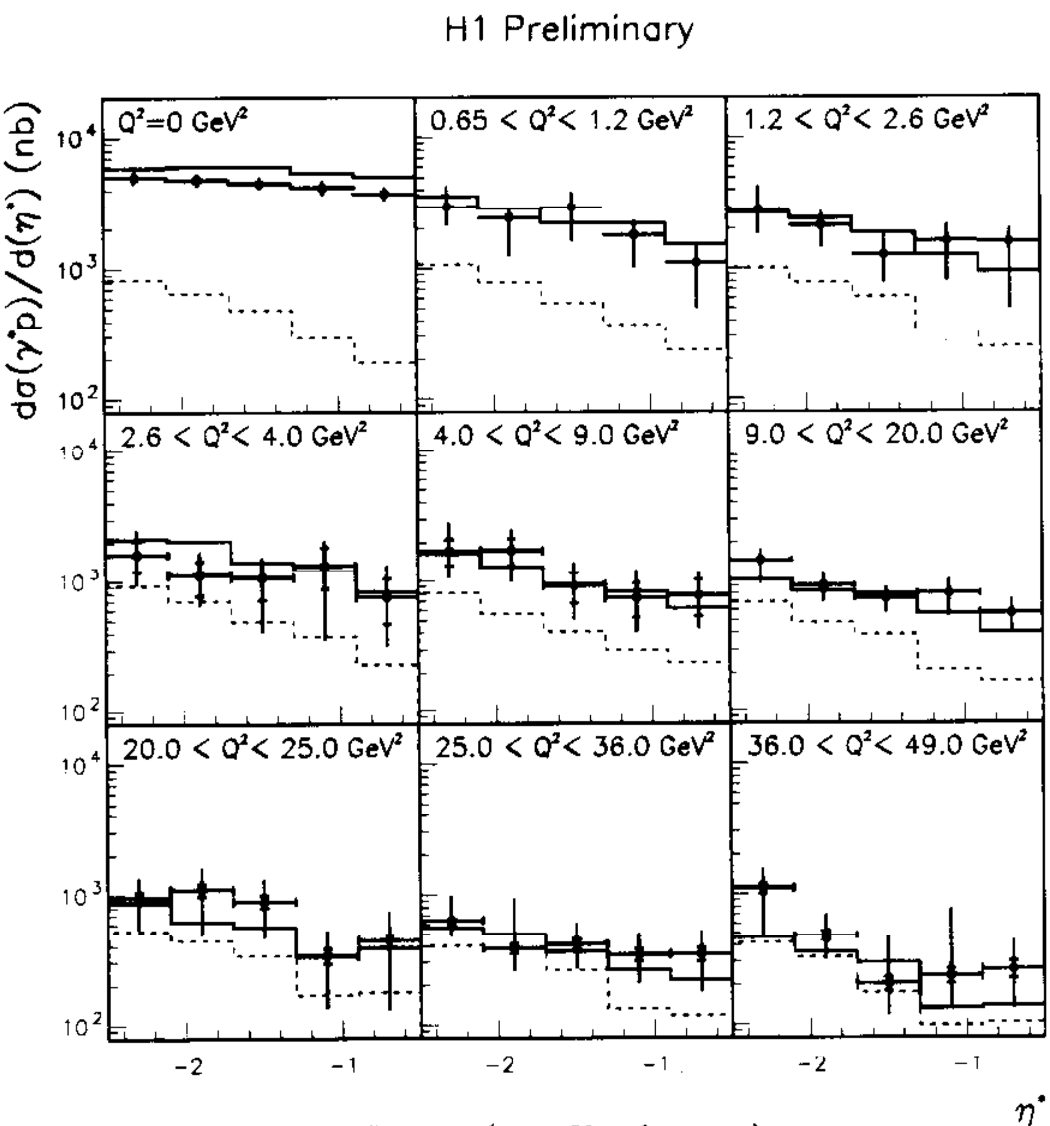

- **H1 Data (preliminary)**
- - - - HERWIG Direct
—— **HERWIG γ^*p Model (Direct+Resolved)**

- Error from Calorimeter Energy Scale shown as band.

$\sigma(Q^2)$

$\gamma^* p$ CROSS-SECTION.

- $-2.5 < \eta^* < -0.5$ and $0.3 < y < 0.6$.

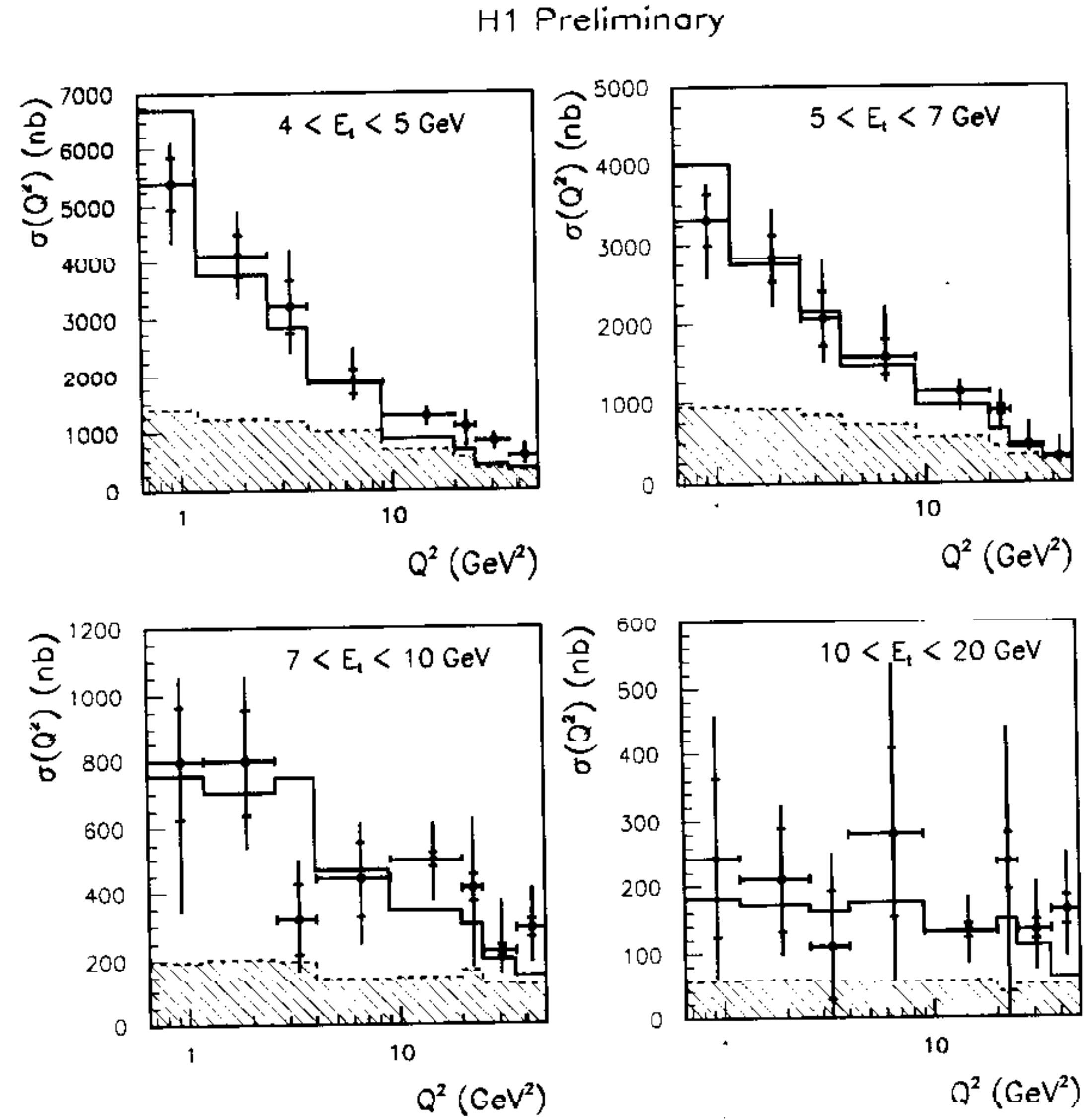

- **H1 Data (preliminary)**
- - - - **HERWIG Direct**
—— **HERWIG γ^*p Model (Direct+Resolved)**

- Error from Calorimeter Energy Scale shown as band.

Photon remnant

- In resolved photon processes, high p_t jets should be accompanied by a photon remnant.
- Jet algorithm reconstructs a photon remnant.
- f is the fraction of the incident photon's energy which is reconstructed in the remnant.
- Data is uncorrected and compared with models after detector simulation.

$$f = \frac{\sum_{\gamma_{rem}} E_i}{E_\gamma}$$

Photon remnant

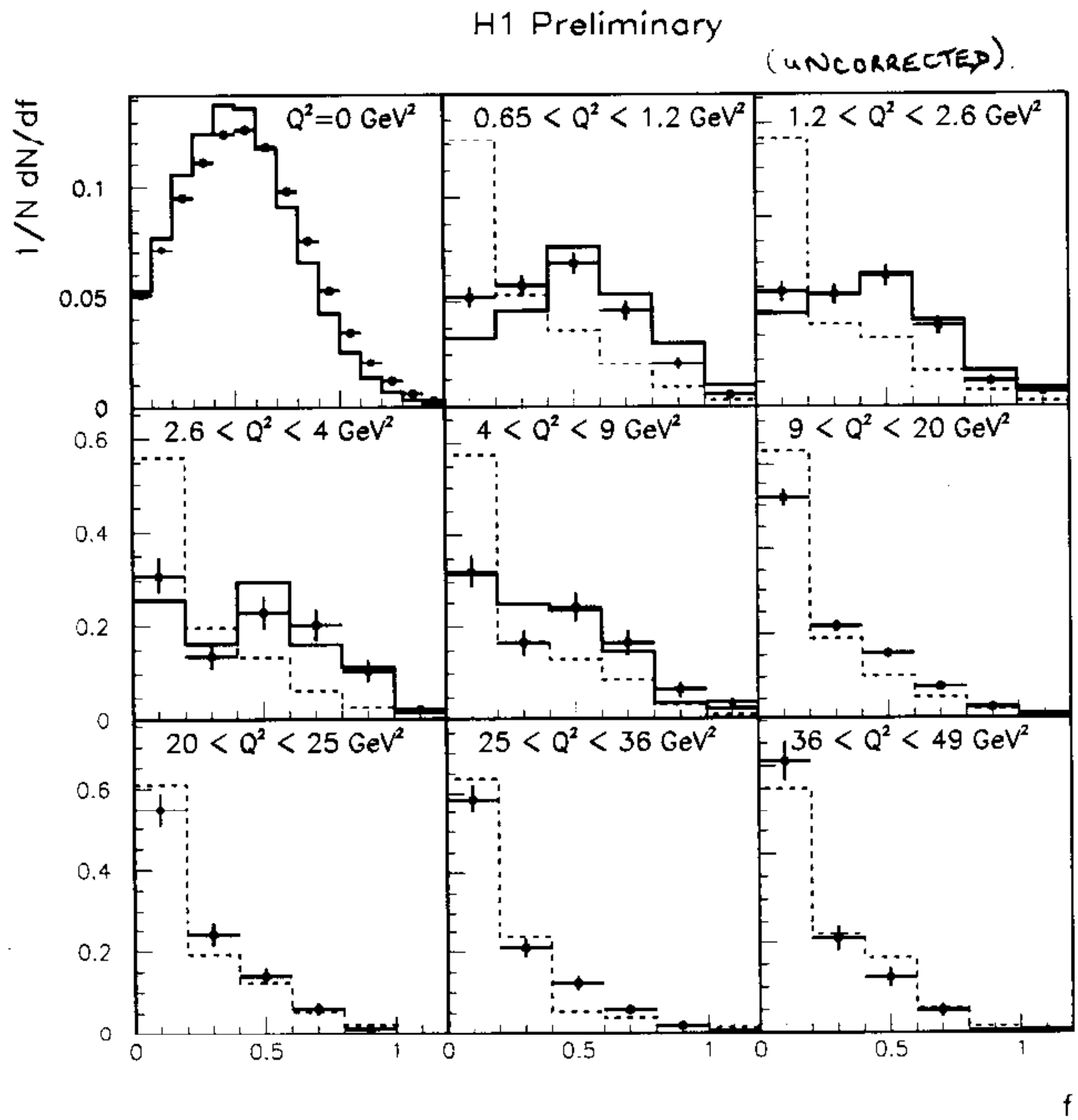

- **H1 Data (preliminary)**
- - - - LEPTO(DIS)
—— **HERWIG γ^*p Model (Direct+Resolved)**

Conclusions

- The single inclusive jet-cross section has been measured for $Q^2 = 0\,\mathrm{GeV}^2$ and $0.65 < Q^2 < 49\,\mathrm{GeV}^2$ with $0.3 < y < 0.6$.
- In the region $p_t^2 >> Q^2$, where the photon can be resolved, the data is inconsistent with a model which treats the photon as a pointlike object
- A phenomenological model which includes a resolved component of the photon suppressed logarithmically with its increasing virtuality describes the data at all Q^2 .
- The energy assigned to the photon remnant is on average large at low Q^2 and decreases with increasing Q^2 , consistent with the picture of a suppressed resolved photon component.